RESEARCH   **Open Access**

CrossMark

Cortical morphological markers in children with autism: a structural magnetic resonance imaging study of thickness, area, volume, and gyrification

Daniel Y.-J. Yang[*], Danielle Beam, Kevin A. Pelphrey, Sebiha Abdullahi and Roger J. Jou

Abstract

Background: Individuals with autism spectrum disorder (ASD) have been characterized by altered cerebral cortical structures; however, the field has yet to identify consistent markers and prior studies have included mostly adolescents and adults. While there are multiple cortical morphological measures, including cortical thickness, surface area, cortical volume, and cortical gyrification, few single studies have examined all these measures. The current study analyzed all of the four measures and focused on pre-adolescent children with ASD.

Methods: We employed the FreeSurfer pipeline to examine surface-based morphometry in 60 high-functioning boys with ASD (mean age = 8.35 years, range = 4–12 years) and 41 gender-, age-, and IQ-matched typically developing (TD) peers (mean age = 8.83 years), while testing for age-by-diagnosis interaction and between-group differences.

Results: During childhood and in specific regions, ASD participants exhibited a lack of normative age-related cortical thinning and volumetric reduction and an abnormal age-related increase in gyrification. Regarding surface area, ASD and TD exhibited statistically comparable age-related development during childhood. Across childhood, ASD relative to TD participants tended to have higher mean levels of gyrification in specific regions. Within ASD, those with higher Social Responsiveness Scale total raw scores tended to have greater age-related increase in gyrification in specific regions during childhood.

Conclusions: ASD is characterized by cortical neuroanatomical abnormalities that are age-, measure-, statistical model-, and region-dependent. The current study is the first to examine the development of all four cortical measures in one of the largest pre-adolescent samples. Strikingly, Neurosynth-based quantitative reverse inference of the surviving clusters suggests that many of the regions identified above are related to social perception, language, self-referential, and action observation networks—those frequently found to be functionally altered in individuals with ASD. The comprehensive, multilevel analyses across a wide range of cortical measures help fill a knowledge gap and present a complex but rich picture of neuroanatomical developmental differences in children with ASD.

Keywords: Autism spectrum disorder, Neuroanatomy, Surface-based morphometry, Brain development, Brain structure

* Correspondence: daniel.yj.yang@yale.edu
Center for Translational Developmental Neuroscience, Child Study Center,
Yale University, New Haven, CT, USA

Yang *et al. Molecular Autism* (2016) 7:11

Page 2 of 14

Background

Autism spectrum disorder (ASD) is a highly prevalent [1], strongly genetic [2], neurodevelopmental disorder, characterized by social and communication impairments as well as repetitive behaviors and restricted interests [3]. Decades of neuroimaging research in ASD have been informative in the search for its complex neurobiology. Numerous fMRI studies have consistently identified atypical brain functioning in a number of regions commonly referred to as the social brain [4–6], including multiple regions within the frontal [7, 8] and temporal cortices [9–12]. Of particular interest is the right posterior superior temporal sulcus (pSTS), which is a central node in social information processing and is functionally disrupted in ASD [6]. On the other hand, the search for neuroanatomical abnormalities via non-diffusion-weighted, structural MRI (sMRI) has yielded less consistent findings, aside from a tendency towards early brain overgrowth during the first years of life [13–16]. The field has yet to identify reliable cortical neuroanatomical markers for ASD using sMRI [17–19]. Moreover, recent studies suggest that neuroanatomical abnormalities in ASD are highly age-dependent [20, 21]. Prior structural neuroimaging research in ASD has included mostly older individuals (adolescents and adults) [22–32], which may not depict an accurate picture about pre-adolescent children with ASD. Among the small number of studies that included children with ASD, many samples consisted of only young children [13, 33, 34], which also may not provide a full picture of the neuroanatomical developmental trajectories in ASD more broadly across childhood. The primary objective of the current study is to address this gap in knowledge by charting cortical developmental differences in a large sample of pre-adolescent children with ASD 4–12 years of age.

We employed a standard processing pipeline of the widely-employed, freely-available FreeSurfer image analysis suite [35] (http://surfer.nmr.mgh.harvard.edu/), which uses surface-based morphometry (SBM), as opposed to voxel-based morphometry (VBM), that reconstructs and characterizes key information about brain structure. It provides better alignment of cortical landmarks than volume-based registration and does not result in an age-associated bias between older and younger children when registering children's brains to a common space [36]. These qualities make FreeSurfer an ideal tool for accurately comparing the brain anatomy of pre-adolescent children.

By reconstructing the brain using spatially fine-grained 3D surface meshes via vertices [37–39], FreeSurfer offers a wide range of cortical structural measures, including cortical thickness (CT), surface area (SA), cortical volume (CV), and cortical gyrification (CG). These measures are correlated with different aspects of cerebral cortical microstructure and are briefly reviewed here. By definition, CV is the product of its two main constituents: CT and SA. It has been widely documented that neurons within the cerebral cortex are modularly organized into ontogenetic columns perpendicular to the surface of the brain [40]. According to the radial unit hypothesis [41], CT is determined by the number of neurons within a column, whereas SA is determined by the number of columns. Furthermore, CT and SA are believed to be determined by different types of progenitor cells [42]. According to the intermediate progenitor hypothesis [43], intermediate progenitor cells (IPC) produce only neurons through symmetric division at subventricular and intermediate zones; the newborn neurons migrate along radial glial fibers to their final cortical destinations and form ontogenetic columns arranged as radial units. The IPCs as neurogenic transient amplifying cells of the developing cerebral cortex amplify each radial unit to form CT but not SA. In contrast, according to the radial unit hypothesis [41], the early proliferation of radial unit progenitor cells (neuroepithelial founder cells and radial glia, which produce single IPCs through asymmetric division at the apical surface) leads to an increase in the number of ontogenetic columns and thus the size of SA. The subdivision of CV into CT and SA thus allows the evaluation of whether CV differences in ASD [44, 45] are attributable to CT, SA, or both, which in turn provides the basis for further investigation of the corresponding cellular and genetic [46] mechanisms underlying ASD.

Furthermore, CG (also known as gyrus formation and cortical folding) is thought to reflect how the human brain manages the problem of packing a phylogenetically increasing cortical surface area into the limited space of the cranial vault [47, 48]. The question of why the cerebral cortex folds the way it does has puzzled the field for a long time. There are a number of interacting, non-mutually exclusive hypotheses of cortical folding in the literature [49]. One of the most influential views is the axonal tension hypothesis [50], which posits that axonal tension between cortical regions induces folding by pulling on the cortex, which draws together regions that are strongly connected and creates folding. This hypothesis is supported by the close relationship between CG and greater local neural connectivity [48, 51]. In contrast, the differential tangential expansion hypothesis [52, 53] postulates that the outer, superficial cortical layers expand more rapidly than the inner, deep cortical layers, which causes cortical folding. Still, a recent synthesized viewpoint [49] suggests that the radial intercalation of young cortical neurons into the outer layer of the developing cortical plate may cause the cortical plate to expand tangentially more rapidly than the underlying tissue, which in turn leads to cortical folding. It is currently unclear which of these hypotheses is more correct, while each of

Yang *et al. Molecular Autism* (2016) 7:11

Page 3 of 14

these hypotheses may generate new directions of investigation about CG development in ASD. In individuals with ASD, CG has been reported to be altered in several areas including the frontal [51, 54, 55] and temporal-occipital regions [56].

Because all of the four cortical measures likely provide unique and complementary information about brain structure and are associated with differential genetic and cellular mechanisms in the brain, it is important to include all of them in the same study of ASD, as a more comprehensive picture is likely to emerge. To our knowledge, no study to date has examined all of these four measures in a predominantly pre-adolescent group of children with ASD. For this reason, we used SBM and examined CT, SA, CV, and CG in one of the largest samples of pre-adolescent children with ASD and a group of typically developing (TD) children who were well-matched on gender, age, and IQ. With the large sample and a comprehensive set of vertex-based cortical morphometric measures, we aim to better understand the neurodevelopmental brain structural differences in ASD during childhood.

Methods

Participants
Study participants included 101 children (all males) between 4 and 12 years of age. They consisted of 60 boys with ASD (4.49–11.99 years) and 41 TD boys (4.75–12.16 years). IQ was characterized using the General Conceptual Ability score of the Differential Ability Scales-Second Edition (DAS-II) [57]. All participants were high-functioning (IQ > 70) ($FSIQ_{ASD}$ = 78–136; $FSIQ_{TD}$ = 78–140). As shown in Table 1, the ASD and TD groups were well-matched on age and IQ.

All participants with ASD met DSM-IV [58] diagnostic criteria for Asperger's syndrome, pervasive developmental disorder—not otherwise specified, or autistic disorder as determined by expert clinical judgment. This judgment was supported by the results of gold standard diagnostic instruments, ADI-R [59] and/or ADOS [60], administered by research-reliable and licensed clinical psychologists. Autistic traits were measured using the parent-reported Social Responsiveness Scale (SRS) total raw score [61]. The complete characterization of the ASD group is reported in Table 2.

To rule out possible developmental delays/disorders and the Broad Autism Phenotype (BAP) [62, 63] in the TD participants, the following exclusionary criteria were used: (1) diagnosed or suspected ASD, schizophrenia, other developmental or psychiatric/neurological disorder; (2) first- or second-degree relative with diagnosed or suspected ASD; (3) an Individualized Education Program for special education services, including speech/language therapy, occupational therapy, and/or social skills intervention; (4) SRS-parent total *t*-score ≥ 76 (severe range); or (5) clinical impression of ASD, other developmental delay/disorder, BAP, or psychiatric disorder.

Exclusion criteria for all participants included seizures (owing to safety concerns during MRI scans), and a history of serious head injury or loss of consciousness. All participants passed MRI safety screening, including being free of any metal implants and evidence of claustrophobia. Written informed consent was obtained from each participant's parent(s), and verbal assent was obtained from each participant. The Human Investigations Committee at Yale University approved this study.

Structural imaging parameters
A high-resolution, T1-weighted, structural imaging sequence was obtained on a 3-Tesla Siemens Tim Trio scanner using a 32-channel head coil and MPRAGE pulse sequence (160 sagittal slices; slice thickness = 1 mm; repetition time = 1900 ms; echo time = 2.96 ms; number of excitations = 1; flip angle = 9°; inversion time = 900 ms; field of view = 256^2 mm²; matrix = 256^2; voxel size = 1.0 mm³).

Cortical reconstruction
FreeSurfer image analysis suite version 5.1.0 (http://surfer.nmr.mgh.harvard.edu/) was employed to perform semi-automated cortical reconstruction. The technical details of these procedures are well-documented in prior publications [64, 65]. In one of the first stages, FreeSurfer registers the individual scans to the MNI305 atlas [66]. Afterwards, FreeSurfer constructs the boundary between white matter and cortical gray matter (this boundary is called the white surface) and the boundary between the gray matter and cerebrospinal fluid/dura (this boundary is called the pial surface). After these 3D surfaces are constructed, CT is estimated as the shortest distance from the

Table 1 Participant demographics and group matching

Variable	TD (n = 41)	ASD (n = 60)	Dx		Age × Dx	
			$t_{(99)}$	p	$F_{(1,97)}$	p
Age	8.83 (2.30)	8.35 (2.07)	1.09	0.28	–	–
General Conceptual Ability IQ	107.00 (15.02)	103.12 (14.51)	1.30	0.20	0.33	0.57
Verbal IQ	107.93 (12.20)	103.77 (17.18)	1.34	0.19	0.23	0.63
Non-verbal IQ	105.37 (15.33)	102.35 (13.82)	1.03	0.31	0.31	0.58

Table 2 ASD group characteristics

Variable	Mean (SD)
ADI-R (n = 56)	
Social	20.50 (5.86)
Verbal communication	16.55 (4.59)
Repetitive	5.95 (2.32)
ADOS Module 2 (n = 2)	
Social affect	13.00 (2.83)
Repetitive behaviors	5.00 (0.00)
Total	18.00 (2.83)
ADOS Module 3 (n = 58)	
Social affect	10.07 (3.47)
Repetitive behaviors	2.74 (1.74)
Total	12.81 (4.12)
ADOS Calibrated Severity score (n = 60)	7.43 (1.74)
SRS-parent total raw score (n = 58)	94.98 (30.30)

white surface to the pial surface at each surface vertex. SA is measured by assigning an area to each vertex equal to the average of its surrounding triangles on the white surface [67]. CV is measured by the amount of gray matter volume that lies between the white surface and the pial surface [68]. CG is measured by the amount of cortex buried within the sulcal folds as compared with the amount of cortex on the outer visible cortex. As computed in FreeSurfer with additional flags [39], CG is quantified by a local gyrification index (LGI) in a 3D space, which is an extension of the 2D gyrification index originally proposed by Ziilles et al. [69]. For example, a LGI of 2.7 means that there is 2.7 times more cortical surface invaginated within the sulci in the surrounding area than the amount of visible cortical surface, while a LGI of 1 means that the cortex is flat in the surrounding area [70]. Most of the reconstruction procedure is automated and has been validated against histological analysis [71] and manual measurement [72]. The structural measures are created using spatial intensity gradients across tissue classes (not restricted to the voxel resolution of the original data) and are capable of detecting sub-millimeter differences.

Quality assurance

In order to prevent any biases or confounds due to Free-Surfer version (workstation type or operating system version) [73], all reconstruction and segmentation computations were performed using computers of exactly the same workstation type and operating system (Dell PowerEdge M610 running CentOS 5.4) on the Yale High-Performance Computing cluster. Quality assurance of the reconstruction was achieved by visually inspecting the data from every participant. Two of the authors (DY and RJ) independently examined the structural MRI

scans for ghosting and blurring. The inspection was performed with only the subject's ID number, so that the raters were blind to information regarding diagnostic group, age, and IQ. Seven scans (6 ASD and 1 TD) were excluded because of severe ghosting/blurring due to head motion.

Analytic approach

We performed group comparisons via GLM analyses using FreeSurfer in a two-step, step-down analytical approach. Age was demeaned in all analyses to ensure that results of the between-group difference refer to anatomy at mean age of the sample rather than age = 0 years. In the first step, we tested an age-by-diagnosis linear age interaction model using the DODS ("different offset, different slope") method and the following GLM equation at every vertex: measure = $b_0 + b_1 \times$ age + $b_2 \times$ diagnosis + $b_3 \times$ age $\times$ diagnosis + error. The goal of the first step is to identify clusters of significant age-by-diagnosis interaction (that is, b_3). In the second step, we screened out the clusters identified in the first step (if any) and tested everywhere else in the cortex using a simpler, between-group main effect model (that is, without the interaction term), the DOSS ("different offset, same slope") method, and the following GLM equation: measure = $b_0 + b_1 \times$ age + $b_2 \times$ diagnosis + error. The goal of the second step is to identify clusters of significant between-group difference independent of age (that is, b_2). This step-down approach ensures that the clusters of significant between-group difference would not confound age-by-diagnosis interaction and thus increases the interpretability of the results. The DOSS method was used to ensure that no interaction term was erroneously included in the second step. The dependent variables were the four cortical structural measures: CT, SA, CV, and CG, respectively. For CT, SA, and CV, a smoothing kernel of 15-mm FWHM was implemented. For CG, because the LGI as implemented in FreeSurfer is already smooth by default, no smoothing kernel (FWHM = 0 mm) was implemented. All analyses were performed on each hemisphere separately. To correct for multiple comparisons and identify significant clusters, a cluster analysis (Monte Carlo null-Z simulation) [74] was implemented at a threshold of $p < 0.05$, two-sided. The statistics for the surviving clusters were reported (e.g., size of the cluster, cluster p value, peak vertex t-statistic, peak vertex coordinates in the Talairach space), while scatterplots (for age-by-diagnosis interaction effects) or boxplots (for diagnosis main effects) were generated to facilitate interpretation of the effects.

Within the ASD group, we performed similar two-step, step-down GLM analyses with the SRS total raw score as a continuous measure of autistic traits. Age and SRS total raw scores were demeaned in all analyses.

Yang *et al. Molecular Autism* (2016) 7:11

Page 5 of 14

In the first step, we tested an age-by-SRS total raw score linear age interaction model using the DODS ("different offset, different slope") method and the following GLM equation at every vertex: measure = $b_0 + b_1 \times$ age $+ b_2 \times$ SRS $+ b_3 \times$ age $\times$ SRS + error. The goal of the first step is to identify clusters of significant age-by-SRS interaction (that is, b_3). In the second step, we screened out the clusters identified in the first step (if any) and tested everywhere else in the cortex using a simpler, main effect model (that is, without the interaction term), the DOSS method, and the following GLM equation: measure = $b_0 + b_1 \times$ age $+ b_2 \times$ SRS + error. The goal of the second step is to identify clusters of a significant main effect of SRS total raw score that is independent of age (that is, b_2). All the other procedures were the same as those used in the group comparison analyses.

To assess the degree to which there is a group difference on global brain anatomy (e.g., [13, 75]), we compared the two groups on several global measures, including total cortical gray matter volume, total cortical white matter volume, subcortical gray matter volume, total gray matter volume, and intra-cranial volume. As seen in Table 3, the two groups of participants were matched for all of these measures, ps > 0.72. This finding of global brain anatomy is similar to that from a previous study including preschool-aged children [33]. Furthermore, there was no significant age-by-diagnosis interaction on these global measures, ps > 0.05. That is, the two groups exhibited statistically comparable trajectories of global brain development. This is also the case for IQ (see Table 1). Together, these findings suggest that controlling for global brain measures or IQ in our data is not warranted and would also reduce power. Thus, we conducted the GLM analyses without controlling for global brain anatomy and IQ.

Meta-analytical reverse inference
To understand the functional relevance of the surviving clusters, we performed a quantitative reverse inference using Neurosynth (http://www.neurosynth.org/). At the time of this research, the Neurosynth dataset v0.5

contains activation data for over 10,900 studies and feature information for over 3300 term-based features. The term-based features were derived from the abstracts of articles in the Neurosynth database. For each feature, the database stores the whole-brain, reverse inference, meta-analysis map, P(Term|Activation), that is, the likelihood that a feature term is used in a study given the presence of reported activation [76]. For each effect of interest (e.g., significant age-by-diagnosis interaction effect) and for each cortical measure (e.g., CT), we merged the surface label files generated by FreeSurfer across all surviving clusters and then converted them to whole-brain volumetric NIfTI files in the standard space (MNI152) via *mri_label2vol*, a tool provided in the FreeSurfer package. Each of these NIfTI files was then decoded with Neurosynth, which computed the voxel-wise Pearson correlation between the input image file and the meta-analytical image file associated with each of the 3300 feature terms. The top 10 functional terms (e.g., spatial, working memory) with the highest positive correlation were retained and reported, while we omitted non-functional terms, such as (but not limited to) those describing an anatomical region (e.g., dorsolateral prefrontal), a technique (e.g., positron emission), or being relatively generic (e.g., task, valid, viewed).
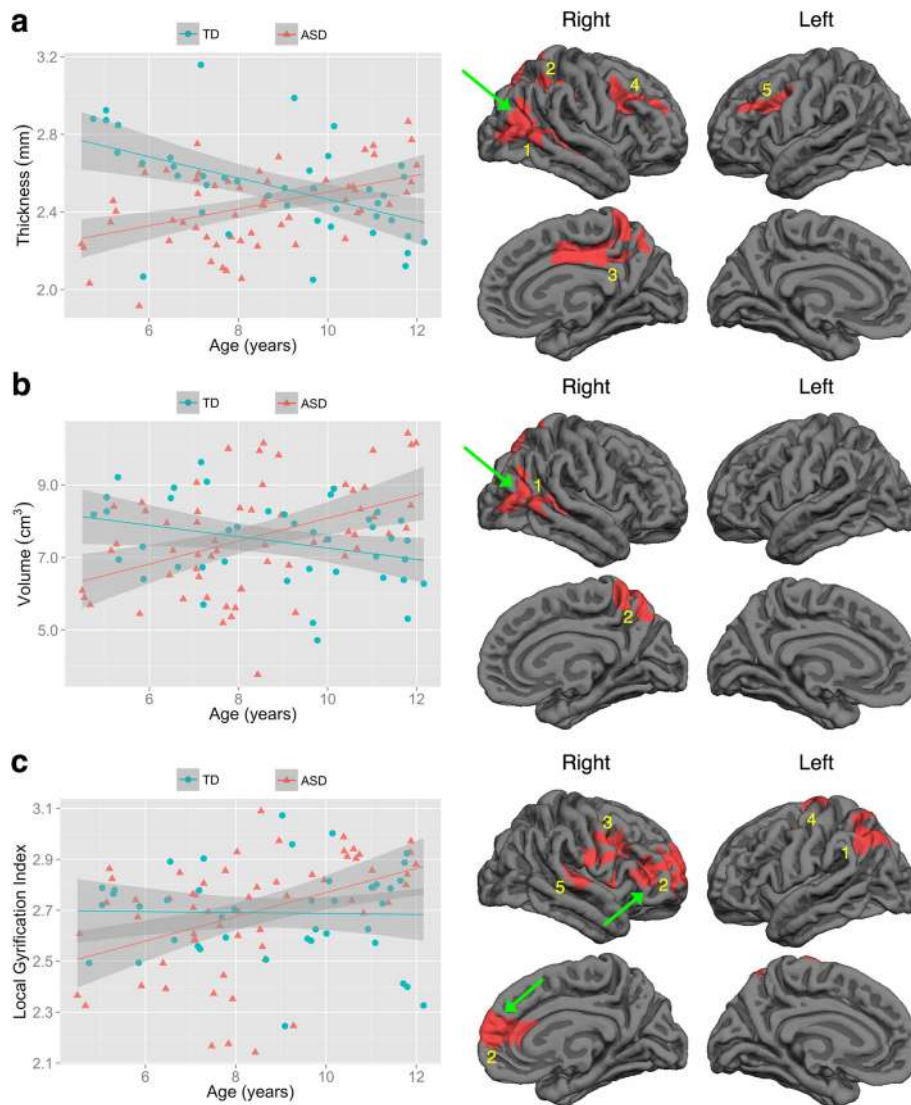
Results
Step 1: age-by-diagnosis interaction effects
The first step of the two-step, step-down GLM analyses revealed several clusters of significant age-by-diagnosis interaction effects on CT, CV, and CG but not SA. As illustrated by representative scatterplots in Fig. 1, on CT, ASD relative to TD exhibited a lack of normative age-related cortical thinning during childhood in several regions, with the peaks found in the right middle temporal, superior parietal, posterior cingulate, rostral middle frontal, and the left caudal middle frontal gyri. On SA, ASD and TD exhibited statistically comparable developmental trajectories. On CV, ASD relative to TD exhibited a lack of normative age-related reduction during childhood in gray matter volume in several regions, with

Table 3 Comparison of global brain anatomy between TD and ASD

Global measure	TD	ASD	Dx $t_{(99)}$	p	Age × Dx $F_{(1,97)}$	p
Cortical gray matter volume	477.79 (53.40)	476.49 (63.94)	0.11	0.92	3.38	0.07
Cortical white matter volume	437.69 (62.19)	434.02 (53.59)	0.32	0.75	0.12	0.73
Subcortical gray matter volume	194.13 (17.27)	193.18 (15.96)	0.29	0.78	0.01	0.92
Total gray matter volume	671.92 (64.18)	669.67 (71.47)	0.16	0.87	2.53	0.12
Intra-cranial volume	1318.38 (157.41)	1328.06 (108.79)	−0.37	0.72	0.11	0.74

The unit is cubic centimeters

Yang *et al. Molecular Autism* (2016) 7:11

Page 6 of 14

Fig. 1 Clusters exhibiting significant age-by-diagnosis interaction effects on **a** cortical thickness, **b** cortical volume, and **c** cortical gyrification. The effects are illustrated by representative scatterplots. Results were corrected for multiple comparisons using cluster analysis, $p < 0.05$, two-sided. There were no surviving clusters for surface area. The numeric labels indicate distinct clusters, and the corresponding information associated with each cluster can be found in the tables. *Dark gray* = sulci; *light gray* = gyri

the peaks found in the right banks of the superior temporal sulcus and the right superior parietal gyrus. Finally, on CG, ASD relative to TD tended to have abnormal age-related increase during childhood in several regions, with the peaks found in the left superior parietal, precentral, right rostral middle frontal, pars opercularis, and superior temporal gyri. Information about all clusters is reported in Table 4 (top), while comprehensive information concerning each cluster is reported in Additional file 1: Figures S1–S3 and Table S1.

Step 2: diagnosis main effects (independent of age)

The second step of the GLM analyses revealed several clusters of significant between-group difference effects independent of age on CG but not CT, SA, and CV. As illustrated by a representative boxplot in Fig. 2, ASD relative to TD tended to have higher mean levels of gyrification in several regions when covarying for age across childhood. The peaks were localized to the right inferior parietal, inferior temporal, lingual, and the left isthmus cingulate gyri. Information about all clusters is reported in Table 4 (bottom), while

Yang *et al. Molecular Autism* (2016) 7:11

Page 7 of 14

Table 4 Clusters of significant differences in cortical morphometry between TD and ASD

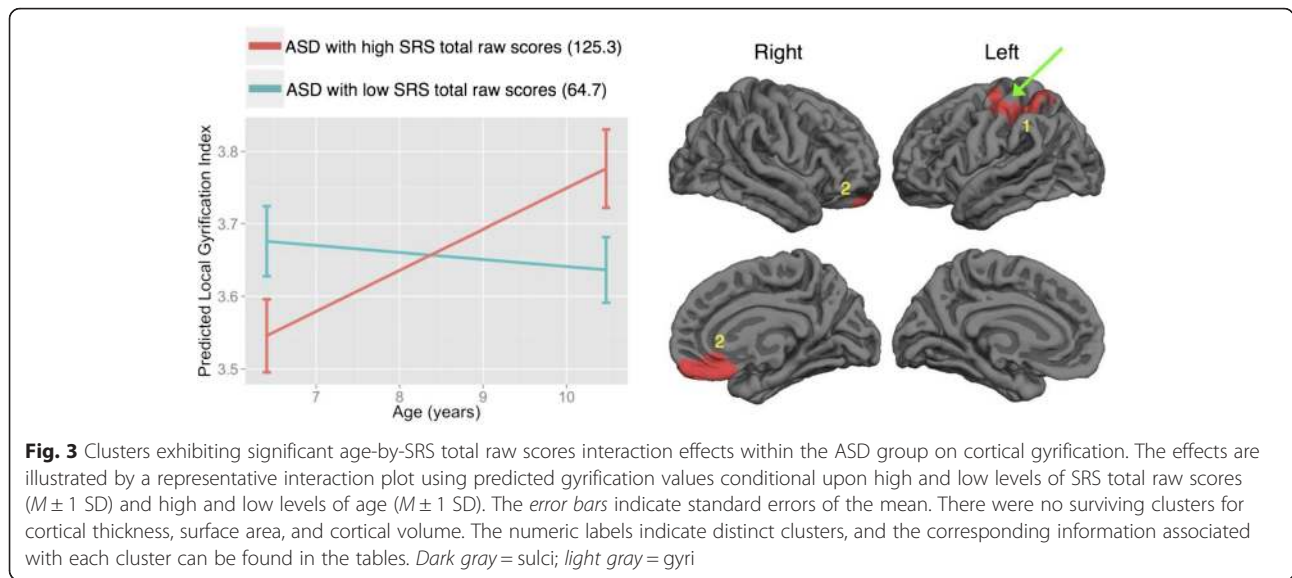| Measure	Cluster	Size (mm²)	$N_{vertices}$	$p_{cluster}$	t_{peak}	X_{Tal}	Y_{Tal}	Z_{Tal}	Peak region
Age-by-diagnosis interaction effects ($df = 97$)									
Thickness	1	2965.01	5623	0.0002	4.334	50.3	−56.7	8.2	R middle temporal
	2	2864.20	6405	0.0002	3.867	19.0	−64.6	43.5	R superior parietal
	3	2558.92	6841	0.0005	4.743	14.6	−14.4	37.4	R posterior cingulate
	4	1878.90	3472	0.0080	3.750	26.5	36.7	18.1	R rostral middle frontal
	5	1457.79	2597	0.0375	3.885	−33.0	9.4	28.1	L caudal middle frontal
Volume	1	2370.44	4619	0.0002	4.677	48.1	−33.0	4.5	R bankssts
	2	1912.43	4245	0.0015	3.658	18.8	−64.9	43.6	R superior parietal
Gyrification	1	2662.70	6064	0.0001	3.361	−27.8	−49.8	48.5	L superior parietal
	2	4359.25	6920	0.0001	3.277	20.2	58.7	8.9	R rostral middle frontal
	3	2141.64	4528	0.0001	3.243	35.6	8.4	21.8	R pars opercularis
	4	995.32	2324	0.0013	3.586	−17.2	−13.4	57.9	L precentral
	5	824.99	1881	0.0067	3.047	64.9	−20.1	2.4	R superior temporal
Between-group differences (independent of Age) ($df = 98$)									
Gyrification	1	2275.23	3856	0.0001	3.862	38.9	−78.1	20.8	R inferior parietal
	2	1625.12	2784	0.0001	3.820	51.2	−13.5	−30.5	R inferior temporal
	3	4186.02	7911	0.0001	3.645	−13.5	−48.8	6.2	L isthmus cingulate
	4	1738.54	2122	0.0001	3.644	10.4	−91.7	−1.7	R lingual

comprehensive information concerning each cluster is reported in Additional file 1: Figure S4.

Analyses of autistic traits within the ASD group
The first step of the two-step, step-down GLM analyses within the ASD group revealed two clusters of significant age-by-SRS total raw score interaction effects on CG but not CT, SA, or CV. As illustrated by a representative interaction plot in Fig. 3 using predicted gyrification values conditional upon high and low levels of SRS total raw scores ($M \pm 1$ SD) and high and low levels of age ($M \pm 1$ SD), those with higher SRS total raw scores (125.3) relative to those with lower SRS total raw scores (64.7) within the ASD group tended to have greater age-related increase in gyrification in specific regions during childhood. The peaks were found in the left precentral and the right medial orbitofrontal gyri. There were no surviving clusters from the second step of the GLM analyses. Information about both clusters is reported in Table 5, while comprehensive information concerning

Fig. 2 Clusters exhibiting significant between-group differences independent of age on cortical gyrification. The effects are illustrated by a representative boxplot. Results were corrected for multiple comparisons using cluster analysis, $p < 0.05$, two-sided. There were no surviving clusters for cortical thickness, surface area, and cortical volume. The numeric labels indicate distinct clusters, and the corresponding information associated with each cluster can be found in the tables. *Dark gray* = sulci; *light gray* = gyri

Fig. 3 Clusters exhibiting significant age-by-SRS total raw scores interaction effects within the ASD group on cortical gyrification. The effects are illustrated by a representative interaction plot using predicted gyrification values conditional upon high and low levels of SRS total raw scores ($M \pm 1$ SD) and high and low levels of age ($M \pm 1$ SD). The *error bars* indicate standard errors of the mean. There were no surviving clusters for cortical thickness, surface area, and cortical volume. The numeric labels indicate distinct clusters, and the corresponding information associated with each cluster can be found in the tables. *Dark gray* = sulci; *light gray* = gyri

each cluster is reported in Additional file 1: Figure S5 and Table S2.

Discussion

The study sets out to examine the cortical morphological differences in a large sample of children with ASD, 4–12 years of age, across all four SBM measures: CT, SA, CV, and CG. Currently, there have been relatively few neuroanatomical studies examining children with ASD in this age range and even fewer studies included all of the four measures at the same time. Our results showed that while there was no age-by-group interaction or between-group difference on global brain anatomy, there were significant age-by-group interactions and between-group differences on regional brain anatomy in CT, CV, and CG but not SA. Our principal findings also held when global brain anatomy (e.g., intracranial volume) and IQ were included as covariates, either separately or together. To interpret the functional relevance of the surviving clusters, we conducted a Neurosynth-based quantitative reverse inference (see Table 6; image files available at http://neurovault.org/collections/1073/; interested readers may decode the image files with NeuroSynth through links within the NeuroVault website). Strikingly, many of the clusters are related to social perception, language, self-referential, and action observation networks—those frequently found to be functionally altered in individuals with ASD [6, 77, 78]. In brief, these neurodevelopmental structural differences

and the use of multiple cortical measures may contribute to a more comprehensive picture of the underlying processes of the social communication difficulties that characterize children with ASD.

Age-by-diagnosis interaction effects

The results showed that ASD relative to TD showed a lack of normative age-related reduction in CT [79] and CV in specific regions during childhood. A closer look at the regions (see Additional file 1: Table S1) reveals that ASD also had abnormal, age-related expansion in CT and CV in specific regions, particularly near the right middle temporal gyrus and the posterior superior temporal sulcus. Recently, there were two longitudinal studies that showed an increase in age-related reduction in CT in ASD during adolescence [21, 80] and on the surface, their findings may appear to be at odds with ours. The discrepancies between these works and ours are summarized here. In the study of Zielinski et al. (2014) [21], the sample consisted of not just children but also many adolescents and adults (age range was 3–36 years; mean age at scan 1 was 15 years) and quadratic age effects were modeled. Thus, their findings during childhood likely reflect a portion of the quadratic age effect across a much wider age range and can have been heavily influenced by the non-linear development in adolescence and then adulthood. Statistically speaking, the quadratic age effect allows only one turning point in the developmental trajectory, which appears to be around

Table 5 Clusters of significant age-by-SRS total raw score interaction on cortical gyrification within ASD

Measure	Cluster	Size (mm²)	N_{vertices}	p_{cluster}	$t_{\text{peak(54)}}$	X_{Tal}	Y_{Tal}	Z_{Tal}	Peak region
Gyrification	1	2950.74	7125	0.0001	3.415	−28.5	−10.3	50.4	L precentral
	2	1319.11	2542	0.0001	2.803	7.6	53.5	−18.7	R medial orbitofrontal

Yang *et al. Molecular Autism* (2016) 7:11

Page 9 of 14

Table 6 Quantitative reverse inference of the surviving clusters using Neurosynth

Measure	Top 10 Neurosynth-decoded feature terms
Clusters of significant age-by-diagnosis interaction effects	
Thickness	Spatial (0.11), working memory (0.10), visuospatial (0.10), attentional (0.09), biological (0.08), motion (0.08), attention (0.07), action observation (0.07), moving (0.07), location (0.06)
Volume	Biological (0.15), motion (0.15), spatial (0.12), location (0.12), orienting (0.11), moving (0.11), visuospatial (0.11), perception (0.10), facial expression (0.09), gaze (0.09)
Gyrification	Pitch (0.09), working memory (0.09), production (0.08), sound (0.07), tone (0.07), vocal (0.07), executive function (0.07), speech production (0.07), audiovisual (0.07), noises (0.06)
Clusters of significant between-group differences (independent of age)	
Gyrification	Navigation (0.08), autobiographical memory (0.08), episodic (0.08), motion (0.07), memories (0.06), relational (0.06), semantic memory (0.06), self-referential (0.04), interpersonal (0.04), mental states (0.04)
Clusters of significant age-by-SRS total raw score interaction effects within ASD	
Gyrification	Hand (0.22), finger (0.22), grasping (0.22), movements (0.18), execution (0.17), action (0.15), motion imagery (0.10), reaching (0.10), touch (0.08), action observation (0.07)

The numbers within the parentheses are correlation coefficients between the surviving clusters and the meta-analysis maps of the feature terms in Neurosynth

late adolescence and early adulthood in their study. We suspect that if a cubic age effect had been modeled, which statistically allows two turning points in the developmental trajectory (e.g., around early adolescence and around early adulthood, respectively [81]), the age effect during childhood in this previous study might have been more similar to ours. Similarly, a recent volumetric analysis including individuals with ASD 3–35 years of age [45] found accelerated decreases in volumes in ASD with age and suggested that the quadratic age effects are primarily due to decreases during late adolescence and adulthood. In contrast, our model fits just the children data using a linear age effect model and captures the childhood phenomena via a different developmental window and statistical model. In addition, in both studies of Wallace et al. (2015) [80] and Zielinski et al. (2014) [21], the main finding is that there is an increase in age-related cortical thinning in ASD during adolescence. This finding is not necessarily in conflict with our finding. Coupled with our finding, the overall picture suggests that abnormal cortical thickening and a lack of age-related normative cortical thinning in ASD during childhood (our finding) is unlikely to continue indefinitely and may be followed by a rebound effect of increased cortical thinning in ASD during adolescence (the findings in both previous studies). In brief, the findings that seem to be in conflict on the surface may have deeper meaningful connections that can prompt new investigations. Future studies should collect a longitudinal sample with more children, a wider age range, and more data time points to further examine this possibility.

In contrast, there was no group difference in the linear developmental trajectory in SA. Despite a null finding, it is consistent with previous research that included adolescents [56] and adolescents and adults [80]. Currently, there is a relative dearth of studies that examine SA. Among them, the significant findings have been mixed and inconsistent. For example, studies that used younger subjects (e.g., aged 0–5 years) found that at an early age, the ASD group has increased SA [13, 82], a study that used adult subjects showed reduced SA [83], but a recent longitudinal study that included children, adolescents, and adults found that the ASD group relative to controls had reduced SA during childhood and increased SA during adulthood in specific regions [84]. Clearly, more work is needed here to unveil the dynamic developmental patterns of surface area in ASD relative to normative developmental patterns.

On CG, the ASD group relative to TD showed an abnormal age-related increase of cortical folding in a number of regions in the right prefrontal lobe, the right temporal lobe, and the left parietal lobe. Within the ASD group, those with higher autistic traits also exhibited age-related CG increase in the right prefrontal lobe and the left parietal lobe. There are currently few studies that have examined developmental trajectories in CG in ASD. More work is also needed here to understand the CG developmental patterns in ASD, relative to normative patterns. Importantly, CG is thought to be associated with local neural connectivity in childhood and adolescence [48]. Our finding of accelerated expansion of CG in the frontal cortex is thus in line with a view that there is local over-connectivity in the frontal cortex in ASD [85]. Furthermore, previous research that included older subjects (adolescents and adults) demonstrated an age-related decrease of cortical folding in ASD but no change in TD [54]. Together with our results, these results suggest that CG in TD is largely a constant from childhood to adulthood [48, 86], while ASD may have abnormal, age-related CG increase during childhood, which is followed by abnormal, age-related CG decline during adolescence and adulthood. In sum, the ASD group relative to TD showed altered developmental trajectories in CT, CV, and CG, suggesting

Yang *et al. Molecular Autism* (2016) 7:11

Page 10 of 14

age-related brain structural dysmaturation in childhood in ASD.

Diagnosis main effects (independent of age)

Our results showed that the ASD group relative to TD had higher mean levels of CG independent of age in the temporal, parietal, and occipital lobes and part of the cingulate cortex, which is consistent with the previous findings of increased CG in ASD [54, 56]. Greater CG is found to be related to greater local connectivity [51], suggesting that the ASD group may have local hyperconnectivity in these regions [87]. It is important to note that our two-step, step-down approach helps to clarify whether the regions are about between-group difference or age-by-diagnosis interactions. This procedure ensures that the between-group difference regions are not moderated by age and can be clearly interpreted. The CG results are highly region-specific, that is, different regions showed age-by-diagnosis interactions or between-group differences. More work is needed to understand the nature of the specific regions of CG increase in ASD.

There were no surviving regions that showed between-group difference in CT, SA, or CV. In light of the age-by-diagnosis findings, our results suggest that the CT and CV cortical differences in ASD during childhood are primarily dynamic, age-dependent, and unfolded in the developmental trajectories over time. A previous similar study by Raznahan et al. (2013) [33] found that children with ASD showed age-independent thicker cortices in specific regions across 2 to 5 years of age. In contrast, the current work included children with ASD 4 to 12 years of age but we did not identify any region that showed mean-level CT difference independent of age. It is possible that there is a cohort effect and also there may be an effect of a wider vs. narrower age range. That is, a wider age range might afford more of the opportunity to examine age-dependent dynamic differences, whereas a narrower age range might inherently limit the results to the static, age-independent, mean-level differences. Future work should include a sample of a wider age range to further understand the discrepancies in these findings.

The importance of using multiple cortical measures

Using all four key cortical measures in a surface-based morphometry study, our results demonstrate the importance of understanding the neuroanatomical basis of ASD using multiple cortical measures. These four measures likely have distinct genetic, environmental, cellular, and biomechanic determinants. Our finding of the ASD difference in the linear developmental trajectories in CV tends to be more similar to that in CT than in SA, suggesting that the CV developmental difference in ASD during childhood may be largely attributable to CT,

rather than SA. In light of the radial unit hypothesis [41], our CT findings suggest that individuals with ASD may fail to have normative age-related reduction in the number or even size of the neuronal cell bodies within the cortical minicolumns in specific cortical regions during childhood. In contrast, our SA finding does not support that individuals with ASD may have abnormal proliferation or decline in the numbers of cortical minicolumns during childhood.

Our CG findings are similar to the CT and CV findings in that ASD participants generally exhibited abnormal age-related increase across these cortical matrices during childhood. However, the CG findings also provide unique information about ASD abnormality. In our results, CG is the only measure that not only showed ASD vs. TD difference in neurodevelopmental trajectory but also captured ASD vs. TD difference in the age-independent mean neuroanatomical difference across childhood and the age-related neuroanatomical abnormality associated with higher levels of autistic traits within the ASD group. This implies that CG may serve as a highly sensitive indicator of ASD abnormality across multiple levels of analysis. Nonetheless, CG differences were seen in a different set of cortical regions (vs. CT and CV) and CG does not replace the roles of CT and CG measures. Currently, there are scant CG works in the literature and more CG work should been done in the future in order to more fully understand the meaning and the underlying cause of the ASD difference in this cortical measure. In summary, it is highly beneficial and important to understand ASD via all four cortical measures, which help to chart a fuller picture of the complexity of ASD and may generate novel and useful hypotheses and research directions.

Limitations

Several limitations of this study are important to consider. First, quality assurance relied on careful visual inspection and data elimination. However, it is likely that individuals with ASD who exhibit more severe symptoms would also find it harder to remain still in the MRI scanner for a long period of time and thus there may be a selection bias in our data. Future research should employ real-time prospective motion correction (PMC) techniques (e.g., [88–90]) during the sMRI scan. The use of PMC techniques can also prevent the risk of using sedation, is more likely to be approved by most IRB for research purpose, and may be a better option than sedation for future sMRI research that aims at minimizing head motion confounds [91]. Second, our data are cross-sectional in nature and the results from the age-related analyses were based on different individuals. Consequently, our results could not rule out the alternative interpretation that the findings reflect cohort differences,

Yang *et al. Molecular Autism* (2016) 7:11

Page 11 of 14

rather than true developmental trajectories, although our TD results of cortical thinning with age are highly congruent with established findings [79]. Future studies should use longitudinal data to further establish the findings. Third, our sample consisted of predominantly high-functioning children with ASD and it remains unclear whether the findings can generalize to children with ASD who show mild to severe intellectual disability. To address this issue, future studies should include individuals with intellectual disability in both the ASD and control groups. Fourth, this study only examined linear age effects and interactions. However, key cortical measures such as CT have been shown to develop in a highly non-linear fashion [81] and recent research has begun to unveil quadratic age-related neurodevelopmental difference in CT in ASD [21, 84]. To properly test the quadratic and also cubic age effects, it would require a sample of a much wider age range than the current sample (e.g., three age cohorts: 4–12, 12–18, and 18–25 years of age, and a large enough number of participants in each age cohort). A minimum of four time points in a longitudinal study has been suggested to be required for reliable quadratic trajectories at the individual level with a cohort sequential sampling design [92]. In contrast, the current sample included exclusively children 4–12 years of age. While it provides a developmental window to test the linear age effect, our sample is not well-suited to carry out the non-linear age-related statistical tests. Future studies should collect a much larger sample of a wider age range to test these more complicated age effects. Finally, the current study only included boys. While males with ASD outnumber females with ASD in the population, our results may be only applicable to male children with ASD because there is a sex difference in the brain structural development [93]. It is important for future studies to collect structural MRI data on female children with ASD to characterize any gender-specific neuroanatomical differences in children with ASD.

Conclusions

The current study is the first to examine cortical thickness, surface area, cortical volume, and cortical gyrification in the same study that included pre-adolescent children with ASD. In addition to rigorous characterization in ASD participants, this study includes a TD comparison group that was well-matched on sex, age, and IQ, which help to minimize possible confounds. The four cortical morphological measures describe a complex but rich picture of the neurodevelopmental structural differences in ASD in this age range. Our sample sizes are relatively large, with 60 participants in ASD and 41 participants in TD, which increase the reliability of the results and the statistical power to detect true effects in MRI studies, especially in

heterogeneous populations such as ASD [94]. Given the known challenges of heterogeneity in the ASD population, future studies should continue to recruit large-scale samples to ensure greater reliability and reproducibility of results. Moreover, being a lifetime neurodevelopmental disorder, future studies should collect longitudinal data at different time points across the lifespan from infancy to late adulthood and apply the approach of multiple morphological measures to help depict a more comprehensive picture of ASD.

Additional file

Abbreviations

Competing interests

Authors' contributions

DY conceived of the study, prepared the data, analyzed the data, and drafted and revised the manuscript. DB helped to analyze the data and helped to draft the manuscript. KP participated in the design of the study and helped to draft and revise the manuscript. SA helped to revise the manuscript. RJ participated in the design of the study, helped to prepare the data, and helped to draft and revise the manuscript. All authors read and approved the final manuscript.

Yang *et al. Molecular Autism* (2016) 7:11

Page 12 of 14

References

1. Blumberg SJ, Bramlett MD, Kogan MD, Schieve LA, Jones JR, Lu MC. Changes in prevalence of parent-reported autism spectrum disorder in school-aged U.S. children: 2007 to 2011-2012. Natl Health Stat Rep. 2013;65:1–11. 1 p following.
2. Abrahams BS, Geschwind DH. Advances in autism genetics: on the threshold of a new neurobiology (vol 9, pg 341, 2008). Nat Rev Genet. 2008;9(6):493.
3. APA. Diagnostic and statistical manual of mental disorders: DSM-5. 5th ed. Washington, D.C: American Psychiatric Publishing; 2013.
4. Minshew NJ, Keller TA. The nature of brain dysfunction in autism: functional brain imaging studies. Curr Opin Neurol. 2010;23(2):124–30. doi:10.1097/WCO.0b013e32833782d4.
5. Philip RC, Dauvermann MR, Whalley HC, Baynham K, Lawrie SM, Stanfield AC. A systematic review and meta-analysis of the fMRI investigation of autism spectrum disorders. Neurosci Biobehav Rev. 2012;36(2):901–42. doi:10.1016/j.neubiorev.2011.10.008.
6. Yang DY, Rosenblau G, Keifer C, Pelphrey KA. An integrative neural model of social perception, action observation, and theory of mind. Neurosci Biobehav Rev. 2015;51:263–75. doi:10.1016/j.neubiorev.2015.01.020.
7. Bookheimer SY, Wang AT, Scott A, Sigman M, Dapretto M. Frontal contributions to face processing differences in autism: evidence from fMRI of inverted face processing. J Int Neuropsychol Soc. 2008;14(6):922–32. doi:10.1017/S135561770808140X.
8. Sabbagh MA. Understanding orbitofrontal contributions to theory-of-mind reasoning: implications for autism. Brain Cogn. 2004;55(1):209–19. doi:10.1016/j.bandc.2003.04.002.
9. Dakin S, Frith U. Vagaries of visual perception in autism. Neuron. 2005;48(3):497–507. doi:10.1016/j.neuron.2005.10.018.
10. Frith U. Mind blindness and the brain in autism. Neuron. 2001;32(6):969–79.
11. Pelphrey KA, Morris JP, McCarthy G. Neural basis of eye gaze processing deficits in autism. Brain. 2005;128(Pt 5):1038–48. doi:10.1093/brain/awh404.
12. Schultz RT, Gauthier I, Klin A, Fulbright RK, Anderson AW, Volkmar F, et al. Abnormal ventral temporal cortical activity during face discrimination among individuals with autism and Asperger syndrome. Arch Gen Psychiatry. 2000;57(4):331–40.
13. Hazlett HC, Poe MD, Gerig G, Styner M, Chappell C, Smith RG, et al. Early brain overgrowth in autism associated with an increase in cortical surface area before age 2 years. Arch Gen Psychiatry. 2011;68(5):467–76. doi:10.1001/archgenpsychiatry.2011.39.
14. Hazlett HC, Poe M, Gerig G, Smith RG, Provenzale J, Ross A, et al. Magnetic resonance imaging and head circumference study of brain size in autism: birth through age 2 years. Arch Gen Psychiatry. 2005;62(12):1366–76. doi:10.1001/archpsyc.62.12.1366.
15. Courchesne E, Karns CM, Davis HR, Ziccardi R, Carper RA, Tigue ZD, et al. Unusual brain growth patterns in early life in patients with autistic disorder: an MRI study. Neurology. 2001;57(2):245–54.
16. Courchesne E, Pierce K, Schumann CM, Redcay E, Buckwalter JA, Kennedy DP, et al. Mapping early brain development in autism. Neuron. 2007;56(2):399–413. doi:10.1016/j.neuron.2007.10.016.
17. Anagnostou E, Taylor MJ. Review of neuroimaging in autism spectrum disorders: what have we learned and where we go from here. Mol Autism. 2011;2(1):4. doi:10.1186/2040-2392-2-4.
18. Chen R, Jiao Y, Herskovits EH. Structural MRI in autism spectrum disorder. Pediatr Res. 2011;69(5 Pt 2):63R–8. doi:10.1203/PDR.0b013e318212c2b3.
19. Amaral DG, Schumann CM, Nordahl CW. Neuroanatomy of autism. Trends Neurosci. 2008;31(3):137–45. doi:10.1016/j.tins.2007.12.005.
20. Lin HY, Ni HC, Lai MC, Tseng WYI, Gau SSF. Regional brain volume differences between males with and without autism spectrum disorder are highly age-dependent. Molecular Autism. 2015;6. doi:10.1186/s13229-015-0022-3.
21. Zielinski BA, Prigge MB, Nielsen JA, Froehlich AL, Abildskov TJ, Anderson JS, et al. Longitudinal changes in cortical thickness in autism and typical development. Brain. 2014;137(Pt 6):1799–812. doi:10.1093/brain/awu083.
22. Hadjikhani N, Joseph RM, Snyder J, Tager-Flusberg H. Anatomical differences in the mirror neuron system and social cognition network in autism. Cereb Cortex. 2006;16(9):1276–82. doi:10.1093/cercor/bhj069.
23. Libero LE, DeRamus TP, Deshpande HD, Kana RK. Surface-based morphometry of the cortical architecture of autism spectrum disorders: volume, thickness, area, and gyrification. Neuropsychologia. 2014;62:1–10. doi:10.1016/j.neuropsychologia.2014.07.001.
24. Ecker C, Marquand A, Mourao-Miranda J, Johnston P, Daly EM, Brammer MJ, et al. Describing the brain in autism in five dimensions–magnetic resonance imaging-assisted diagnosis of autism spectrum disorder using a multiparameter classification approach. J Neurosci. 2010;30(32):10612–23. doi:10.1523/JNEUROSCI.5413-09.2010.
25. Hyde KL, Samson F, Evans AC, Mottron L. Neuroanatomical differences in brain areas implicated in perceptual and other core features of autism revealed by cortical thickness analysis and voxel-based morphometry. Hum Brain Mapp. 2010;31(4):556–66. doi:10.1002/hbm.20887.
26. Raznahan A, Toro R, Daly E, Robertson D, Murphy C, Deeley Q, et al. Cortical anatomy in autism spectrum disorder: an in vivo MRI study on the effect of age. Cereb Cortex. 2010;20(6):1332–40. doi:10.1093/cercor/bhp198.
27. Wallace GL, Dankner N, Kenworthy L, Giedd JN, Martin A. Age-related temporal and parietal cortical thinning in autism spectrum disorders. Brain. 2010;133(Pt 12):3745–54. doi:10.1093/brain/awq279.
28. Chung MK, Robbins SM, Dalton KM, Davidson RJ, Alexander AL, Evans AC. Cortical thickness analysis in autism with heat kernel smoothing. Neuroimage. 2005;25(4):1256–65. doi:10.1016/j.neuroimage.2004.12.052.
29. Ecker C, Ginestet C, Feng Y, Johnston P, Lombardo MV, Lai MC, et al. Brain surface anatomy in adults with autism: the relationship between surface area, cortical thickness, and autistic symptoms. JAMA Psychiatry. 2013;70(1):59–70. doi:10.1001/jamapsychiatry.2013.265.
30. Dziobek I, Bahnemann M, Convit A, Heekeren HR. The role of the fusiform-amygdala system in the pathophysiology of autism. Arch Gen Psychiatry. 2010;67(4):397–405. doi:10.1001/archgenpsychiatry.2010.31.
31. Scheel C, Rotarska-Jagiela A, Schilbach L, Lehnhardt FG, Krug B, Vogeley K, et al. Imaging derived cortical thickness reduction in high-functioning autism: key regions and temporal slope. Neuroimage. 2011;58(2):391–400. doi:10.1016/j.neuroimage.2011.06.040.
32. Doyle-Thomas KA, Duerden EG, Taylor MJ, Lerch JP, Soorya LV, Wang AT, et al. Effects of age and symptomatology on cortical thickness in autism spectrum disorders. Res Autism Spectr Disord. 2013;7(1):141–50. doi:10.1016/j.rasd.2012.08.004.
33. Raznahan A, Lenroot R, Thurm A, Gozzi M, Hanley A, Spence SJ, et al. Mapping cortical anatomy in preschool aged children with autism using surface-based morphometry. NeuroImage Clinical. 2012;2:111–9. doi:10.1016/j.nicl.2012.10.005.
34. Schumann CM, Bloss CS, Barnes CC, Wideman GM, Carper RA, Akshoomoff N, et al. Longitudinal magnetic resonance imaging study of cortical development through early childhood in autism. J Neurosci. 2010;30(12):4419–27. doi:10.1523/JNeurosci.5714-09.2010.
35. Fischl B. FreeSurfer. Neuroimage. 2012;62(2):774–81. doi:10.1016/j.neuroimage.2012.01.021.
36. Ghosh SS, Kakunoori S, Augustinack J, Nieto-Castanon A, Kovelman I, Gaab N, et al. Evaluating the validity of volume-based and surface-based brain image registration for developmental cognitive neuroscience studies in children 4 to 11 years of age. Neuroimage. 2010;53(1):85–93. doi:10.1016/j.neuroimage.2010.05.075.
37. Dale AM, Fischl B, Sereno MI. Cortical surface-based analysis. I. Segmentation and surface reconstruction. Neuroimage. 1999;9(2):179–94. doi:10.1006/nimg.1998.0395.
38. Fischl B, Sereno MI, Dale AM. Cortical surface-based analysis. II: Inflation, flattening, and a surface-based coordinate system. Neuroimage. 1999;9(2):195–207. doi:10.1006/nimg.1998.0396.

Yang *et al. Molecular Autism* (2016) 7:11

Page 13 of 14

39. Schaer M, Cuadra MB, Tamarit L, Lazeyras F, Eliez S, Thiran JP. A surface-based approach to quantify local cortical gyrification. IEEE Trans Med Imaging. 2008;27(2):161–70. doi:10.1109/TMI.2007.903576.

40. Mountcastle VB. The columnar organization of the neocortex. Brain. 1997;120(Pt 4):701–22.

41. Rakic P. A small step for the cell, a giant leap for mankind: a hypothesis of neocortical expansion during evolution. Trends Neurosci. 1995;18(9):383–8.

42. Kriegstein A, Noctor S, Martinez-Cerdeno V. Patterns of neural stem and progenitor cell division may underlie evolutionary cortical expansion. Nat Rev Neurosci. 2006;7(11):883–90. doi:10.1038/nrn2008.

43. Pontious A, Kowalczyk T, Englund C, Hevner RF. Role of intermediate progenitor cells in cerebral cortex development. Dev Neurosci. 2008;30(1-3):24–32. doi:10.1159/000109848.

44. Courchesne E, Campbell K, Solso S. Brain growth across the life span in autism: age-specific changes in anatomical pathology. Brain Res. 2011;1380:138–45. doi:10.1016/j.brainres.2010.09.101.

45. Lange N, Travers BG, Bigler ED, Prigge MB, Froehlich AL, Nielsen JA, et al. Longitudinal volumetric brain changes in autism spectrum disorder ages 6–35 years. Autism Res. 2015;8(1):82–93. doi:10.1002/aur.1427.

46. Panizzon MS, Fennema-Notestine C, Eyler LT, Jernigan TL, Prom-Wormley E, Neale M, et al. Distinct genetic influences on cortical surface area and cortical thickness. Cereb Cortex. 2009;19(11):2728–35. doi:10.1093/cercor/bhp026.

47. Schüz A, Miller R. Cortical areas : unity and diversity. London. New York: Taylor & Francis; 2002.

48. White T, Su S, Schmidt M, Kao CY, Sapiro G. The development of gyrification in childhood and adolescence. Brain Cogn. 2010;72(1):36–45. doi:10.1016/j.bandc.2009.10.009.

49. Striedter GF, Srinivasan S, Monuki ES. Cortical folding: when, where, how, and why? Annu Rev Neurosci. 2015;38:291–307. doi:10.1146/annurev-neuro-071714-034128.

50. Van Essen DC. A tension-based theory of morphogenesis and compact wiring in the central nervous system. Nature. 1997;385(6614):313–8. doi:10.1038/385313a0.

51. Schaer M, Ottet MC, Scariati E, Dukes D, Franchini M, Eliez S, et al. Decreased frontal gyrification correlates with altered connectivity in children with autism. Front Hum Neurosci. 2013;7:750. doi:10.3389/fnhum.2013.00750.

52. Ronan L, Voets N, Rua C, Alexander-Bloch A, Hough M, Mackay C, et al. Differential tangential expansion as a mechanism for cortical gyrification. Cereb Cortex. 2014;24(8):2219–28. doi:10.1093/cercor/bht082.

53. Richman DP, Stewart RM, Hutchinson JW, Caviness VS. Mechanical model of brain convolutional development. Science. 1975;189(4196):18–21.

54. Hardan AY, Jou RJ, Keshavan MS, Varma R, Minshew NJ. Increased frontal cortical folding in autism: a preliminary MRI study. Psychiatry Res. 2004;131(3):263–8. doi:10.1016/j.pscychresns.2004.06.001.

55. Jou RJ, Minshew NJ, Keshavan MS, Hardan AY. Cortical gyrification in autistic and Asperger disorders: a preliminary magnetic resonance imaging study. J Child Neurol. 2010;25(12):1462–7. doi:10.1177/0883073810368311.

56. Wallace GL, Robustelli B, Dankner N, Kenworthy L, Giedd JN, Martin A. Increased gyrification, but comparable surface area in adolescents with autism spectrum disorders. Brain. 2013;136(Pt 6):1956–67. doi:10.1093/brain/awt106.

57. Elliott CD. Differential Ability Scale—Second Edition (DAS-II). San Antonio, TX: The Psychological Corporation; 2007.

58. APA. Diagnostic and Statistical Manual of Mental Disorders, 4th ed, text revision (DSM-IV-TR). Washington, DC: American Psychiatric Association; 2000.

59. Lord C, Rutter M, Le Couteur A. Autism Diagnostic Interview-Revised: a revised version of a diagnostic interview for caregivers of individuals with possible pervasive developmental disorders. J Autism Dev Disord. 1994;24(5):659–85.

60. Lord C, Rutter M, Goode S, Heemsbergen J, Jordan H, Mawhood L, et al. Autism diagnostic observation schedule: a standardized observation of communicative and social behavior. J Autism Dev Disord. 1989;19(2):185–212.

61. Constantino JN. The Social Responsiveness Scale. Western Psychological Services: Los Angeles; 2002.

62. Hurley RS, Losh M, Parlier M, Reznick JS, Piven J. The broad autism phenotype questionnaire. J Autism Dev Disord. 2007;37(9):1679–90. doi:10.1007/s10803-006-0299-3.

63. Losh M, Adolphs R, Poe MD, Couture S, Penn D, Baranek GT, et al. Neuropsychological profile of autism and the broad autism phenotype. Arch Gen Psychiatry. 2009;66(5):518–26. doi:10.1001/archgenpsychiatry.2009.34.

64. Fischl B, van der Kouwe A, Destrieux C, Halgren E, Segonne F, Salat DH, et al. Automatically parcellating the human cerebral cortex. Cereb Cortex. 2004;14(1):11–22.

65. Han X, Jovicich J, Salat D, van der Kouwe A, Quinn B, Czanner S, et al. Reliability of MRI-derived measurements of human cerebral cortical thickness: the effects of field strength, scanner upgrade and manufacturer. Neuroimage. 2006;32(1):180–94. doi:10.1016/j.neuroimage.2006.02.051.

66. Collins DL, Neelin P, Peters TM, Evans AC. Automatic 3D intersubject registration of MR volumetric data in standardized Talairach space. J Comput Assist Tomogr. 1994;18(2):192–205.

67. Winkler AM, Sabuncu MR, Yeo BT, Fischl B, Greve DN, Kochunov P, et al. Measuring and comparing brain cortical surface area and other areal quantities. Neuroimage. 2012;61(4):1428–43. doi:10.1016/j.neuroimage.2012.03.026.

68. Winkler AM, Kochunov P, Blangero J, Almasy L, Zilles K, Fox PT, et al. Cortical thickness or grey matter volume? The importance of selecting the phenotype for imaging genetics studies. Neuroimage. 2010;53(3):1135–46. doi:10.1016/j.neuroimage.2009.12.028.

69. Zilles K, Armstrong E, Schleicher A, Kretschmann HJ. The human pattern of gyrification in the cerebral cortex. Anat Embryol (Berl). 1988;179(2):173–9.

70. Schaer M, Cuadra MB, Schmansky N, Fischl B, Thiran JP, Eliez S. How to measure cortical folding from MR images: a step-by-step tutorial to compute local gyrification index. Jove-J Vis Exp. 2012(59). doi:10.3791/3417.

71. Rosas HD, Liu AK, Hersch S, Glessner M, Ferrante RJ, Salat DH, et al. Regional and progressive thinning of the cortical ribbon in Huntington's disease. Neurology. 2002;58(5):695–701.

72. Salat DH, Buckner RL, Snyder AZ, Greve DN, Desikan RS, Busa E, et al. Thinning of the cerebral cortex in aging. Cereb Cortex. 2004;14(7):721–30. doi:10.1093/cercor/bhh032.

73. Gronenschild EH, Habets P, Jacobs HI, Mengelers R, Rozendaal N, van Os J, et al. The effects of FreeSurfer version, workstation type, and Macintosh operating system version on anatomical volume and cortical thickness measurements. Plos One. 2012;7(6), e38234. doi:10.1371/journal.pone.0038234.

74. Hagler Jr DJ, Saygin AP, Sereno MI. Smoothing and cluster thresholding for cortical surface-based group analysis of fMRI data. Neuroimage. 2006;33(4):1093–103. doi:10.1016/j.neuroimage.2006.07.036.

75. Freitag CM, Luders E, Hulst HE, Narr KL, Thompson PM, Toga AW, et al. Total brain volume and corpus callosum size in medication-naive adolescents and young adults with autism spectrum disorder. Biol Psychiatry. 2009;66(4):316–9. doi:10.1016/j.biopsych.2009.03.011.

76. Yarkoni T, Poldrack RA, Nichols TE, Van Essen DC, Wager TD. Large-scale automated synthesis of human functional neuroimaging data. Nat Methods. 2011;8(8):665–70. doi:10.1038/nmeth.1635.

77. Williams DL, Cherkassky VL, Mason RA, Keller TA, Minshew NJ, Just MA. Brain function differences in language processing in children and adults with autism. Autism Res. 2013;6(4):288–302. doi:10.1002/aur.1291.

78. Lombardo MV, Barnes JL, Wheelwright SJ, Baron-Cohen S. Self-referential cognition and empathy in autism. Plos One. 2007;2(9), e883. doi:10.1371/journal.pone.0000883.

79. Sowell ER, Thompson PM, Leonard CM, Welcome SE, Kan E, Toga AW. Longitudinal mapping of cortical thickness and brain growth in normal children. J Neurosci. 2004;24(38):8223–31. doi:10.1523/JNEUROSCI.1798-04.2004.

80. Wallace GL, Eisenberg IW, Robustelli B, Dankner N, Kenworthy L, Giedd JN, et al. Longitudinal cortical development during adolescence and young adulthood in autism spectrum disorder: increased cortical thinning but comparable surface area changes. J Am Acad Child Adolesc Psychiatry. 2015;54(6):464–9. doi:10.1016/j.jaac.2015.03.007.

81. Shaw P, Kabani NJ, Lerch JP, Eckstrand K, Lenroot R, Gogtay N, et al. Neurodevelopmental trajectories of the human cerebral cortex. J Neurosci. 2008;28(14):3586–94. doi:10.1523/Jneurosci.5309-07.2008.

82. Lyall AE, Shi F, Geng X, Woolson S, Li G, Wang L et al. dynamic development of regional cortical thickness and surface area in early childhood. Cereb Cortex. 2014. doi:10.1093/cercor/bhu027.

83. Ecker C, Ginestet C, Feng Y, Johnston P, Lombardo MV, Lai MC, et al. Brain surface anatomy in adults with autism. Jama Psychiatry. 2013;70(1):59–70. doi:10.1001/jamapsychiatry.2013.265.

84. Ecker C, Shahidiani A, Feng Y, Daly E, Murphy C, D'Almeida V, et al. The effect of age, diagnosis, and their interaction on vertex-based measures of cortical thickness and surface area in autism spectrum disorder. J Neural Transm. 2014;121(9):1157–70. doi:10.1007/s00702-014-1207-1.

Yang *et al. Molecular Autism* (2016) 7:11

Page 14 of 14

85. Courchesne E, Pierce K. Why the frontal cortex in autism might be talking only to itself: local over-connectivity but long-distance disconnection. Curr Opin Neurobiol. 2005;15(2):225–30. doi:10.1016/j.conb.2005.03.001.

86. Armstrong E, Schleicher A, Omran H, Curtis M, Zilles K. The ontogeny of human gyrification. Cereb Cortex. 1995;5(1):56–63.

87. Lynch CJ, Uddin LQ, Supekar K, Khouzam A, Phillips J, Menon V. Default mode network in childhood autism: posteromedial cortex heterogeneity and relationship with social deficits. Biol Psychiatry. 2013;74(3):212–9. doi:10.1016/j.biopsych.2012.12.013.

88. Tisdall MD, Hess AT, Reuter M, Meintjes EM, Fischl B, van der Kouwe AJ. Volumetric navigators for prospective motion correction and selective reacquisition in neuroanatomical MRI. Magn Reson Med. 2012;68(2):389–99. doi:10.1002/mrm.23228.

89. Brown TT, Kuperman JM, Erhart M, White NS, Roddey JC, Shankaranarayanan A, et al. Prospective motion correction of high-resolution magnetic resonance imaging data in children. Neuroimage. 2010;53(1):139–45. doi:10.1016/j.neuroimage.2010.06.017.

90. White N, Roddey C, Shankaranarayanan A, Han E, Rettmann D, Santos J, et al. PROMO: real-time prospective motion correction in MRI using image-based tracking. Magn Reson Med. 2010;63(1):91–105. doi:10.1002/mrm.22176.

91. Reuter M, Tisdall MD, Qureshi A, Buckner RL, van der Kouwe AJ, Fischl B. Head motion during MRI acquisition reduces gray matter volume and thickness estimates. Neuroimage. 2015;107:107–15. doi:10.1016/j.neuroimage.2014.12.006.

92. Willett JB, Singer JD, Martin NC. The design and analysis of longitudinal studies of development and psychopathology in context: statistical models and methodological recommendations. Dev Psychopathol. 1998;10(2):395–426.

93. Lenroot RK, Gogtay N, Greenstein DK, Wells EM, Wallace GL, Clasen LS, et al. Sexual dimorphism of brain developmental trajectories during childhood and adolescence. Neuroimage. 2007;36(4):1065–73. doi:10.1016/j.neuroimage.2007.03.053.

94. Button KS, Ioannidis JP, Mokrysz C, Nosek BA, Flint J, Robinson ES, et al. Power failure: why small sample size undermines the reliability of neuroscience. Nat Rev Neurosci. 2013;14(5):365–76. doi:10.1038/nrn3475.